



Published in final edited form as:

Arch Ophthalmol. 2011 November ; 129(11): 1458–1465. doi:10.1001/archophthalmol.2011.330.

Real-Time Ophthalmoscopic Findings of Super-Selective Intra-Ophthalmic Artery Chemotherapy in a Non-Human Primate Model

Matthew W. Wilson, MD, FACS^{1,2,3}, John S. Jackson, DVM⁴, Blanca X. Phillips, COA¹, Jacquelyn Buchanan, COA¹, Sharon Frase³, Fan Wang, PhD⁵, Jena J. Steinle, PhD¹, Clinton F. Stewart, PharmD⁵, Timothy D. Mandrell, DVM⁴, Barrett G. Haik, MD, FACS^{1,2}, and J. Scott Williams, MD, PhD^{6,7}

¹Hamilton Eye Institute, Department of Ophthalmology, University of Tennessee Health Science Center, Memphis, Tennessee

²Department of Surgery, Division of Ophthalmology, St Jude Children's Research Hospital, Memphis, Tennessee

³Department of Pathology, St Jude Children's Research Hospital, Memphis, Tennessee

⁴Department of Comparative Medicine, University of Tennessee Health Science Center, Memphis, Tennessee

⁵Department of Pharmaceutical Sciences, St Jude Children's Research Hospital, Memphis, Tennessee

⁶Department of Radiology, University of Tennessee Health Science Center, Memphis, Tennessee

⁷Department of Radiology, MetroHealth Medical Center, Cleveland, Ohio

Abstract

Objectives—To report real-time ophthalmoscopic findings during super-selective intra-ophthalmic artery chemotherapy (SSIOAC) in a non-human primate (NHP) model.

Methods—Six adult male Rhesus macaques (*Macacca mulatta*) were randomly assigned into one of two treatment cohorts; MEL treated with 5 mg/30 mL melphalan, and CBP treated with 30 mg/30 mL carboplatin. Each animal underwent three separate SSIOAC procedures at three-week intervals. Digital retinal images were obtained during each infusion. Intravenous fluorescein angiography was performed immediately after each procedure.

Results—All SSIOAC procedures were successfully completed. Toxicities were equally distributed between drug cohorts. Systemic toxicities included mild bone marrow suppression in all animals and anorexia in one. One animal had greater than 50% narrowing of the treated ophthalmic artery after its second infusion. All 18 procedures (100%) resulted in pulsatile optic nerve and choroid blanching, retinal artery narrowing, and retinal edema. Retinal artery sheathing was found during 17 (of 18, 94%) procedures, and retinal artery precipitates were seen in 10 (of 18, 56%). Choroidal hypoperfusion (18 of 18, 100%) was seen by fluorescein angiogram.

Conclusions—Real-time ophthalmic investigations are useful and, in our NHP model, indicate prevalent, acute ocular vascular toxicities during SSIOAC.

Clinical Relevance—Real-time retinal imaging is feasible in an NHP model of SSIOAC. Application to SSIOAC in children may shed insight into reported vascular toxicities.

Introduction

With primary systemic chemotherapy moving to the forefront in the treatment of childhood retinoblastoma, progress has been made in saving eyes and vision.^{1–3} Yet, eyes are still lost to extensive disease, and children must endure the associated toxicities of systemic chemotherapy. In 2008, super-selective intra-ocular artery chemotherapy (SSIOAC) was put forth as a means of delivering high intraocular concentrations of chemotherapy to treat extensive disease while minimizing systemic exposure and its resultant toxicities.⁴ In those and further studies there were no reports of adverse central nervous system events, limb loss, or bleeding diathesis.^{4–7} Reported side effects included transient pancytopenia, eyelid erythema and edema, and eyelash loss.^{4–8} Vision-threatening side effects have included ophthalmic artery (OA) thrombosis, retinal detachment and non-clearing vitreous hemorrhage.^{4–13} More recently, delayed choroidal filling has been observed on intravenous fluorescein angiography (IVFA) after SSIOAC.¹⁴

Known mutagenic effects and concentration-dependent toxicities of melphalan (the current chemotherapeutic of choice) are cause for concern.¹⁵ To date, no data regarding ocular drug levels in SSIOAC have been published. Published clinical studies are only now reporting short-term and long-term ocular toxicity.^{4–14} Such limitations have led us to study SSIOAC in a non-human primate (NHP) pre-clinical model. The specific aims of our study were (1) to use real-time ophthalmic imaging to document the acute ocular toxicities during SSIOAC, (2) to measure the vitreous and systemic PK of chemotherapy administered via SSIOAC, (3) to describe the histopathology of NHP eyes treated by SSIOAC, and (4) to validate our NHP model by comparing orbital vascular anatomy to that of a two-year old child. We will address aims 2–4 in subsequent reports. In this, our initial report, we address our first aim and describe real-time observations of SSIOAC in a NHP model and document acute retinal and choroidal vascular toxicities.

Methods

Approval for the study was obtained from the Institutional Animal Care and Use Committee at the University of Tennessee Health Science Center, Memphis, Tennessee. All animals were maintained in an AAALAC accredited facility and treated in accordance with the Guide for the Care and Use of Laboratory Animals,²⁵ and guidelines set forth by the Association for Research in Vision and Ophthalmology.

Six adult male Rhesus macaques (*Macacca mulatta*) were randomly assigned into one of two treatment cohorts, melphalan (MEL, 5 mg/30 mL) or carboplatin (CBP, 30 mg/30 mL).⁴ Each animal underwent three separate SSIOAC procedures spaced at three-week intervals with the right being the treated eye unless prohibited by vascular anomalies. Prior to each procedure a baseline ophthalmic examination inclusive of indirect ophthalmoscopy with sclera depression was performed; digital retinal images were obtained using a RETCAM (Clarity Medical Systems, Pleasanton, CA, USA). The final procedure was terminal.

Under general anesthesia and using sterile technique, percutaneous vascular access was gained through the right femoral artery using a 21-gauge butterfly needle with the animal in a supine position. A 0.018-inch access guidewire was passed through the needle and the needle removed. A 4F microaccess catheter was placed over its matched dilator and the dilator and wire removed. This was positioned in the descending aorta and used as a guide catheter for the microcatheter. The microaccess catheter was attached to a heparinized saline flush at minimal flow rate to maintain patency using a rotating hemostatic valve. A

Marathon® 1.3F microcatheter was placed over a Mirage® 0.08 inch micro-guidewire (both from ev3 Neurovascular, Irvine, CA, USA) and the pair used to selectively catheterize the right common carotid artery using uniplanar fluoroscopy, imaging in the frontal projection (General Electric Health Care, OEC Series 9600, Waukesha, WI). The animal's head was then rotated onto its left side for a lateral projection. The right OA was super-selectively catheterized using the micro-catheter with minimal micro-guidewire manipulation. Nitroglycerine (100 µg/ml) was used as needed to limit flow-restricting vasospasm. A selective ophthalmic arteriogram using Optiray® 320 (Mallinckrodt, Inc., St Louis, MO, USA) was obtained to document position, anatomy and antegrade flow. The designated chemotherapeutic was then infused over 30 minutes by pulsatile manual delivery (1 mL/min). Positioning of the microcatheter was checked fluoroscopically during infusion and post-infusion. The catheter and access sheath were removed and homeostasis obtained using manual pressure.

Upon confirmed access of the OA each drug was prepared, the solution pH was measured, and infusion was performed. Freeze-dried melphalan (50 mg, Bioncheperma, Lake Forest, IL, USA) was reconstituted, per the manufacturers instructions, with 10 mL of sterile diluents (provided by manufacturer) to yield a 5 mg/ml concentration; 1 mL of which was subsequently diluted in 29 mL of normal saline to provide the desired 5 mg/30 mL concentration (5.5 pH). Three milliliters of 10 mg/ml carboplatin solution (APP, Schaumburg, IL, USA) were diluted in 27 mL of normal saline to yield a 30 mg/30 mL concentration (5.0 pH). A 5 mL infusion of vehicle (normal saline, 5.5 pH) was performed immediately prior to drug delivery to serve as internal control following our first two procedures.

Immediately prior to infusion of the chemotherapeutic, a 1200 pediatric RETCAM lens was placed on the cornea of the right eye, and the optic, macula and vascular arcades were imaged to assure flow through the central retinal artery. The lens was left in place through the course of the study and serial images were obtained. Upon completion of the infusion, IVFA was performed using 1ml of 10% fluorescein dye.

Animals were followed daily after SSIOAC treatments by veterinarians. Activity, diet and blood counts were monitored. Weekly ophthalmic examinations were performed under intra-muscular ketamine sedation. Digital external and retinal images were obtained.

Results

The pre-treatment characteristics of the NHPs are listed in Table 1. Each animal was successfully treated with 3 cycles of SSIOAC. The right OA was accessed less than 2 mm distal to its ostium. For 10 of the 18 procedures 1 mL of 100 µg/ml of nitroglycerine was used to minimize potential vasospasm. During the final procedure in CBP 404, narrowing of the OA proximal to the origin of the central retinal artery was observed, necessitating two separate injections of nitroglycerine (Figure 1). As antegrade flow was present, if slowed, we continued with the procedure. The optic nerve maintained normal perfusion through the central retinal artery. No other complications related to arterial access or micro-catheter placements were observed.

The only noted behavioral change was loss of appetite in one primate, which persisted for approximately one week after each procedure. The median weight of the animals did not change throughout the study (11.6 kg, ranges given in Table 1). After the first two treatments, all animals had mild bone marrow suppression, with hematocrits, hemoglobins, and absolute neutrophil counts dipping just below normal range for the species (Table 1).

Baseline ophthalmic examinations were remarkable only for a corneal scar from a prior ulcer in the right eye of MEL 561. The toxicities documented by real-time ophthalmic imaging in nearly all perfusions are shown in Figure 2. During each infusion there was visible pulsatile pallor of the optic nerve (Figures 3 and 4) coincidental with drug delivery. Four (of 18, 22%) procedures had simultaneous choroidal blanching. The choroid and optic nerve re-perfused between each pulsation. Pre-treatment vehicle infusion resulted only in pulsatile changes in the optic nerve. As the infusion progressed we observed narrowing of the retinal arterial with associated sheathing in some cases (as seen in IVFA, Figures 5–7). The inferior temporal and nasal arcades were most often affected.

Precipitates spontaneously appeared in the retinal arteries in 56% (10 of 18, 5 in each cohort) of the procedures, sometimes filling the arterial tree. The extent and duration of the precipitates varied, appearing from 7 to 20 minutes into an infusion. In each instance, there had been antecedent marked narrowing of the retinal arteries with or without associated sheathing of the vessels. What were felt to be coinciding choroidal infarcts were simultaneously seen. The majority of precipitates cleared over minutes, completely resolving by the end of each infusion.

Using IVFA, we saw delayed choroidal filling and persistent areas of non-perfusion following each study (Figures 5–7). The observed choroidal changes differed in severity amongst the procedures and animals, with delays in choroid filling lasting from seconds to minutes. Persistent choroidal non-perfusion was sectoral in nature. In some cases, truncation of the retinal arterial tree and diffuse retinal capillary drop out coincided with delayed filling of the retinal veins.

Interval dilated fundus exams (Figure 8) showed resolution of acute vasculopathies. However, nerve fiber layer infarcts and intra-retinal hemorrhages persisted in most animals between procedures (Figure 9). No persistent optic nerve pallor or orbital toxicities were observed. Persistent right upper eyelid edema and anisocoria (larger treated pupil, no relative difference in pupils between light and dark) were noted in two animals each. A definitive afferent pupillary defect was not documented in either animal.

Discussion

We successfully completed 18 SSIOAC procedures in six NHPs (three per animal). Our NHPs tolerated the procedure with minimal observed systemic toxicities—mild bone marrow suppression in all and anorexia in one. In contrast, ophthalmic vascular toxicities were significant and equally distributed between both cohorts (Figures 2, 5 and 8). Recent studies report similar vasculopathies remote to SSIOAC, including sectoral choroidal occlusive vasculopathy, retinal arteriolar emboli, central and branch retinal artery occlusion, transient vasospasm with visual loss, diffuse exudative angiopathy, and vitreous hemorrhage.^{9–14} Our real-time study suggests the acute ocular vascular toxicities occurring during treatment are significantly greater than those observed at weeks one, two and three post- procedure.

However, we can only monitor the ocular vasculopathy during SSIOAC, the resultant damage to the OA and its branches cannot be discovered until subsequent selective angiograms as we and others have shown (Figure 1).¹⁰ An OA thrombosis was noted in one animal on selective OA angiogram during the final procedure. More than 50% narrowing of the right OA proximal to the origin of the central retinal artery was observed. Interval dilated examinations of the right eye after the second SSIOAC had shown only nerve fiber infarcts and intra-retinal hemorrhages. The central artery was perfused and the optic nerve appeared normal.

We believe that our observed vascular toxicities and those reported in children are best explained by our previously reported¹⁶ *in vitro* studies on cultured human retinal vascular endothelial cells, where a 1 hour exposure to a 4 µg/ml melphalan dose increased cell death by greater than 6-fold. Surviving cells showed a significant increase in migration and proliferation. Up-regulation of inflammatory mediators ICAM-1 and IL-8—both promoters of leukostasis similar to that found in diabetic retinopathy—was seen.¹⁷ Thus the concentrations of melphalan being used for SSIOAC may induce vaso-occlusive disease,¹⁵ which may lead to observed sight-threatening vasculopathies. These vasculopathies may be compounded by the concurrent disruption of blood flow with pulsatile delivery and presence of particulates as we observed. A review of the literature indicates that disruption of blood flow promotes vascular endothelial cell inflammation and apoptosis.¹⁸

The effect of the infused solutions' pH must also be taken into consideration.¹⁹ Most intravenous solutions have an acidic pH, due in part to the delivery vehicle, yet are generally well tolerated. Melphalan and carboplatin (pH 5.5 and 5.0, respectively) are typically infused into large caliber venous vessels minimizing the effect of pH. The effect of an acidic solution on a small caliber artery is not known but should raise concerns similar to those previously voiced regarding acid-induced thrombophlebitis.^{20,21} It should be noted that during infusion of our control vehicle, normal saline (pH of 5.5), no toxicities were observed. No current clinical SSIOAC study has commented on or made reference to solution pH. We believe pH may play an important role in the observed vascular toxicities. The need for pH adjustment and subsequent impact on drug solubility should be addressed.

We must also comment on the retinal arterial precipitates seen in 6 of our animals during 10 different infusions. We used transmission electron microscopy to determine if the observed particles could be precipitates of the chemotherapeutic solution (JEOL 1200 EX Transmission Electron Microscope (Peabody, MA, USA) with a CCD XR 11 camera from Advanced Microscopy Techniques (Wobum, MA, USA). We prepared solution samples in the same manner as for infusion and used them within one hour of preparation. We placed 10 µL of each solution on 300 mesh carbon coated grids and dried them under a hood for 15 minutes. Any excess solution thereafter was wicked away and the grids were allowed to dry. Each solution showed particles—5 µm aggregates in the melphalan and 2 µm crystals in the carboplatin (Figure 10). We do not believe these particles solely account for the retinal artery precipitates. We hypothesize that our findings resulted from a complex interaction amongst inflammatory mediators, leukostasis and the particulates seen on electron microscopy, which could be in keeping with reported retinal arteriole emboli or Roth Spots.¹⁴ Clearly, further investigation is needed.

Lastly, we must address the relevance of our pre-clinical model. Prior studies have shown Rhesus macaques are a valid model to study anti-cancer drug pharmacokinetics, as they are large enough for repeated sampling, inclusive of blood and cerebrospinal fluid.²²⁻²⁴ Furthermore, the size and weight of an adult male Rhesus macaque is comparable to that of a human two year-old, the age of a child most likely to undergo SSIOAC. These similarities provided us a means to better understand the SSIOAC; most notably the acute vascular ocular toxicities we have detailed using real-time ophthalmic imaging throughout the course of infusion.

As an institution, we have not yet adopted SSIOAC for the treatment of intraocular retinoblastoma in our patients. We encourage those who have to investigate the questions we have raised, specifically with regards to acute vascular toxicities, drug concentration, pH, and particulates. In turn, we will pursue our questions in pre-clinical models. In conclusion, we believe we have shown there is considerable merit in documenting real-time observations during SSIOAC.

Acknowledgments

Grant Support: This study was supported in part by an unrestricted grant to the Department of Ophthalmology from Research to Prevent Blindness, Inc, New York, New York, and the St Giles Foundation, New York, New York.

References

1. Shields CL, Shields JA. Diagnosis and management of retinoblastoma. *Cancer Control*. 2004; 11(5): 317–27. [PubMed: 15377991]
2. Chintagumpala M, Chevez-Barrios P, Paysse EA, et al. Retinoblastoma: review of current management. *Oncologist*. 2007; 12(10):1237–46. [PubMed: 17962617]
3. Rodriguez-Galindo C, Chantada GL, Haik BG, Wilson MW. Treatment of retinoblastoma: current status and future perspectives. *Curr Treat Options Neurol*. 2007; 9(4):294–307. [PubMed: 17580009]
4. Abramson DH, Dunkel IJ, Brodie SE, et al. A phase I/II study of direct intraarterial (ophthalmic artery) chemotherapy with melphalan for intraocular retinoblastoma initial results. *Ophthalmology*. 2008; 115(8):1398–1404. [PubMed: 18342944]
5. Abramson DH, Dunkel IJ, Brodie SE, et al. Superselective ophthalmic artery chemotherapy as primary treatment for retinoblastoma (chemosurgery). *Ophthalmology*. 2010; 117(8):1623–9. [PubMed: 20381868]
6. Abramson DH, Dunkel IJ, Brodie SE, et al. Bilateral superselective ophthalmic artery chemotherapy for bilateral retinoblastoma: tandem therapy. *Arch Ophthalmol*. 2010; 128(3):370–2. [PubMed: 20212212]
7. Gobin YP, Dunkel IJ, Marr BP, et al. Intra-arterial chemotherapy for the management of retinoblastoma: Four-year experience. *Arch Ophthalmol*. 2011 Feb 14. [Epub ahead of print].
8. Marr BP, Gobin PY, Dunkel IJ, et al. Spontaneously resolving periocular erythema and ciliary madarosis following intra-arterial chemotherapy for retinoblastoma. *Middle East Afr J Ophthalmol*. 2010; 17(3):207–9. [PubMed: 20844675]
9. Shields CL, Ramasubramanian A, Rosenwasser R, Shields JA. Superselective catheterization of the ophthalmic artery for intraarterial chemotherapy for retinoblastoma. *Retina*. 2009; 29(8):1207–9. [PubMed: 19734768]
10. Shields CL, Shields JA. Intra-arterial chemotherapy for retinoblastoma: The beginning of a long journey. *Clin Experiment Ophthalmol*. 2010; 38(6):638–43. [PubMed: 20584015]
11. Shields CL, Shields JA. Retinoblastoma management: advances in enucleation, intravenous chemoreduction, and intra-arterial chemotherapy. *Curr Opin Ophthalmol*. 2010; 21(3):203–12. [PubMed: 20224400]
12. Vajzovic LM, Murray TG, Aziz-Sultan MA, et al. Supraselective intra-arterial chemotherapy: evaluation of treatment-related complications in advanced retinoblastoma. *Clin Ophthalmol*. 2011; 5:171–6. [PubMed: 21383945]
13. Peterson EC, Elhammady MS, Quintero-Wolfe S, et al. Selective ophthalmic artery infusion of chemotherapy for advanced intraocular retinoblastoma: initial experience with 17 tumors. *J Neurosurg*. 2011 Feb 4. [Epub ahead of print].
14. Munier FL, Beck-Popovic M, Balmer A, et al. Occurrence of sectoral choroidal occlusive vasculopathy and retinal arteriolar embolization after superselective ophthalmic artery chemotherapy for advanced intraocular retinoblastoma. *Retina*. 2011; 31(3):566–73. [PubMed: 21273941]
15. Samuels BL, Bitran JD. High-dose intravenous melphalan: a review. *J Clin Oncol*. 1995; 13(7): 1786–99. [PubMed: 7602368]
16. Wilson, MW.; Zhang, Q.; Steinle, JJ. Exposure of human retinal endothelial cells to high dose chemotherapy upregulates inflammation and chemotaxis. Presented at the annual meeting of the Association for Research in Vision and Ophthalmology; Ft Lauderdale. May 2011;
17. Li J, Jin C, Cleveland JC Jr, et al. Enhanced inflammatory response to toll-like receptor 2/4 stimulation in type 1 diabetic coronary artery endothelial cells: the effect of insulin. *Cardiovasc Diabetol*. 2010; 9:90. [PubMed: 21162749]

18. Walshe TE, Connell P, Cryan L, et al. The role of pulsatile flow in controlling microvascular retinal endothelial and pericyte cell apoptosis and proliferation. *Cardiovasc Res.* 2011; 89(3):661–70. [PubMed: 21030535]
19. Lebowitz MH, Masuda JY, Beckerman JH. The pH and acidity of Intravenous Infusion Solutions. *JAMA.* 1971; 215(12):1937–40. [PubMed: 5107833]
20. Elfving G, Saikku K. Effect of pH on the incidence of infusion thrombophlebitis. *Lancet.* 1966; 1(7444):953. [PubMed: 4160648]
21. Fonkalsrud EW, Murphy JL, Smith FG Jr. Effect of pH in glucose infusions on development of thrombophlebitis. *J Sur Res.* 1968; 8(11):539–43.
22. Berg SL, Aleksic A, McGuffey L, et al. Plasma and cerebrospinal fluid pharmacokinetics of rebeccamycin (NSC 655649) in nonhuman primates. *Cancer Chemother Pharmacol.* 2004; 54(2): 127–30. [PubMed: 15150671]
23. Berg SL, Stone J, Xiao JJ, et al. Plasma and cerebrospinal fluid pharmacokinetics of depsipeptide (FR901228) in nonhuman primates. *Cancer Chemother Pharmacol.* 2004; 54:85–8. [PubMed: 15042312]
24. Berg S, Serabe B, Aleksic A, et al. Pharmacokinetics and cerebrospinal fluid penetration of phenylacetate and phenylbutyrate in the nonhuman primate. *Cancer Chemother Pharmacol.* 2001; 47(5):385–90. [PubMed: 11391852]
25. Institute for Laboratory Animal Research. Guide for the care and use of laboratory animals. Washington (DC): National Academies Press; 1996.

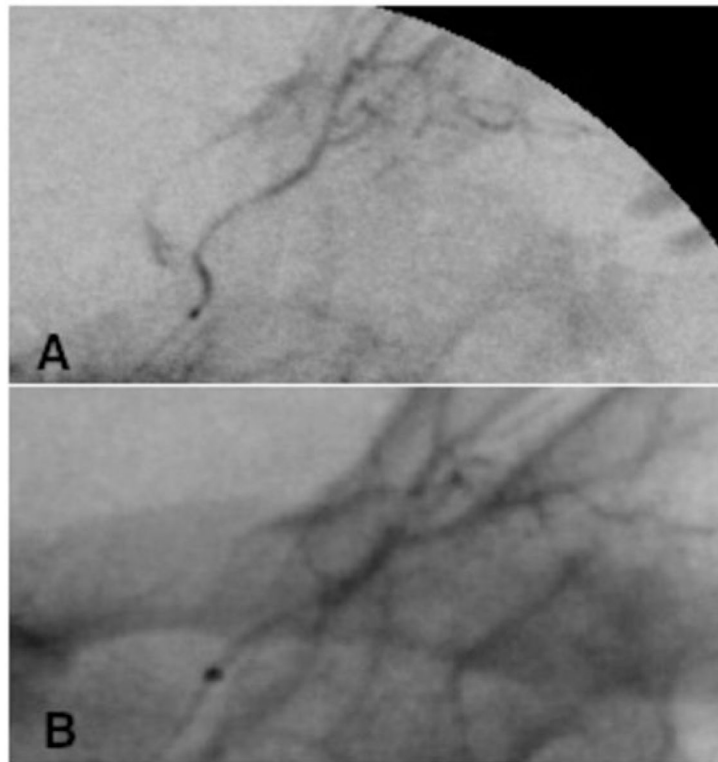


Figure 1. Selective ophthalmic arteriograms from CBP 404 showing (A) successful initial catheterization with patent artery and (B) subsequent narrowing of artery during third infusion.

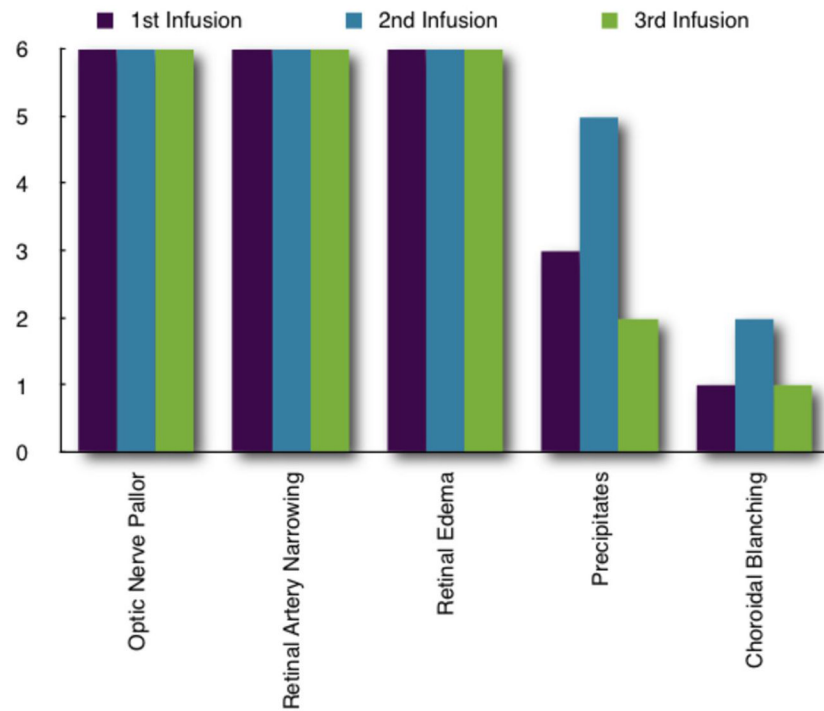


Figure 2. Real-time ophthalmic findings for each infusion in all six animals. Precipitates occurred equally in melphanan and carboplatin cohorts (five instances in both) and in every animal. Three of the four instances of choroidal blanching occurred in one animal in the carboplatin cohort.

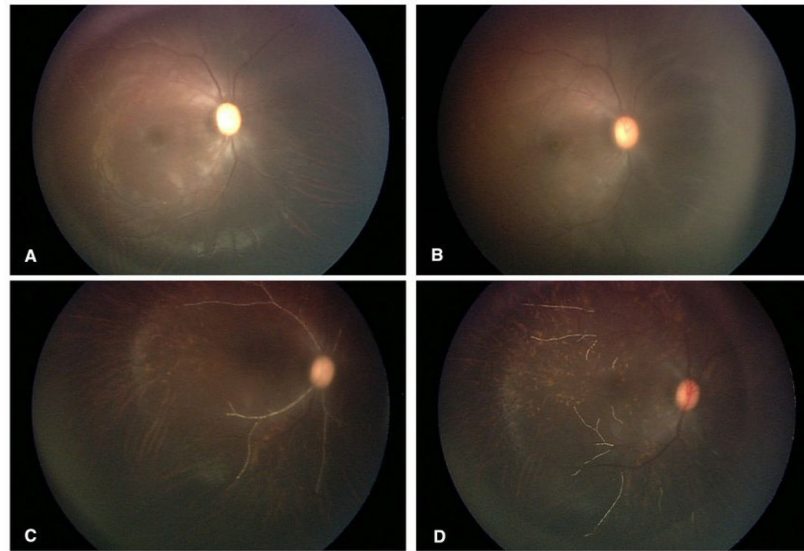


Figure 3. Real time retinal observations during melphalan infusion: (A) pulsatile optic nerve pallor with retinal edema; (B) retinal artery narrowing with loss of inferior temporal and nasal arcades; (C) retinal artery precipitates; (D) clearing precipitates with underlying choroidal abnormalities.

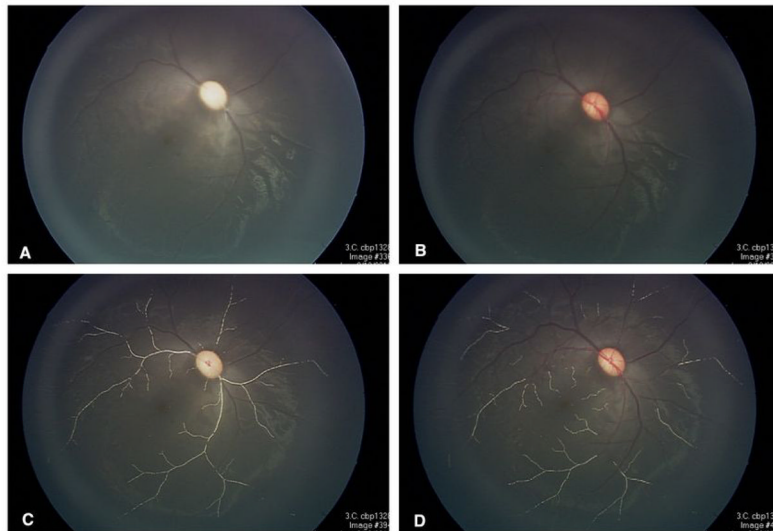


Figure 4. Real time retinal observations during carboplatin infusion: (A) pulsatile optic nerve pallor with retinal edema and narrowing of the retinal arteries; (B) re-perfusion of the optic between pulsations; (C) retinal artery precipitates; (D) clearing of the precipitates with underlying choroidal abnormalities.

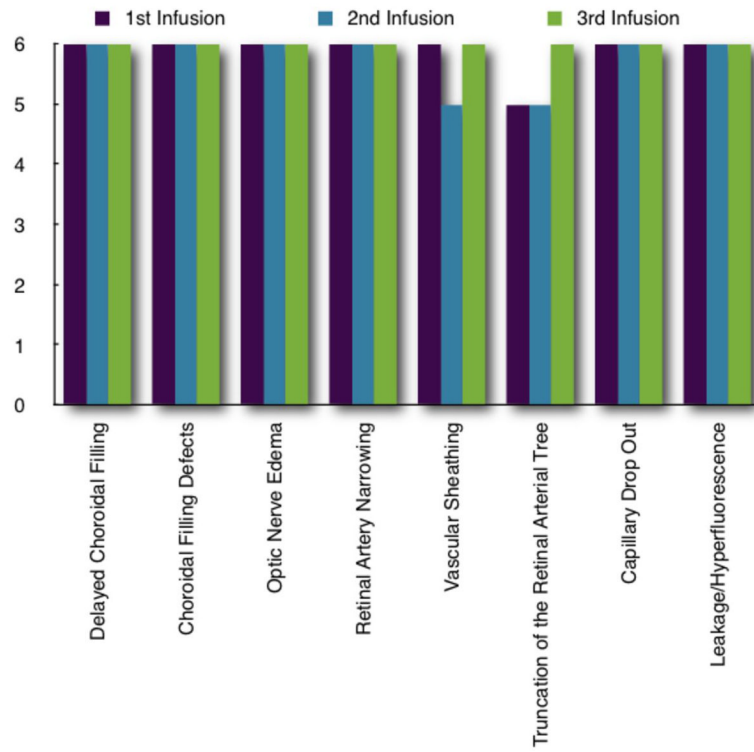


Figure 5. Intravenous fluoroscopic angiography for each infusion in all six animals.

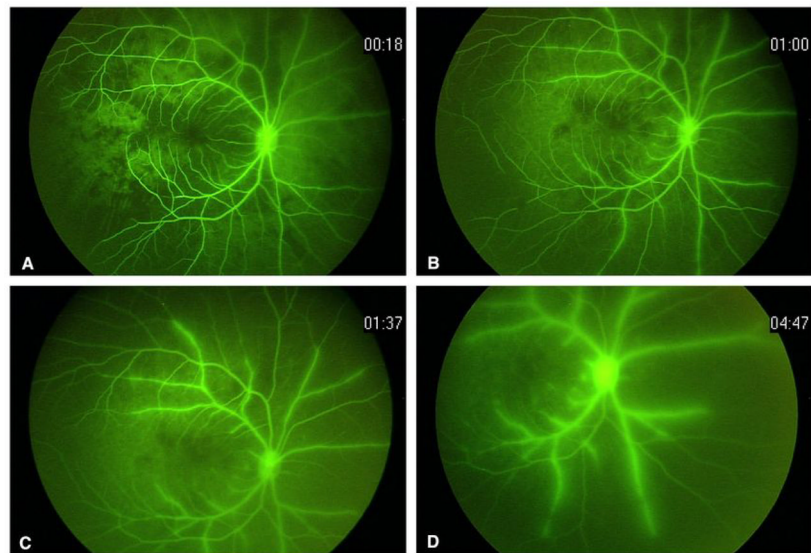


Figure 6. Intravenous fluoroscopic angiography corresponding to Figure 3: (A) delayed, sectoral choroidal filling; (B) persistent areas of choroidal non-perfusion with early artery sheathing and diffuse capillary dropout; (C) persistent sheathing of the arteries, early optic hyperfluorescence and leakage from parafoveal vessels; (D) late frame showing progressive sheathing, leakage, optic nerve hyperfluorescence and hypoperfusion of the nasal choroid and retina.

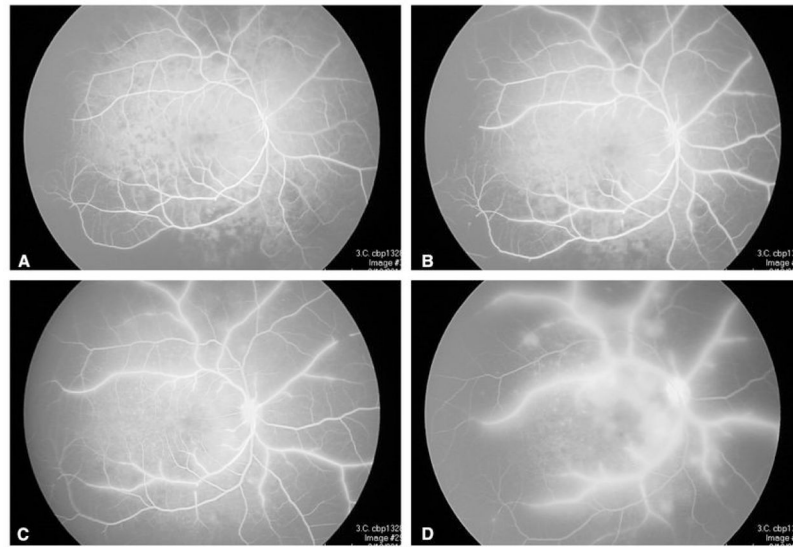


Figure 7. Intravenous fluorescein angiography corresponding to Figure 4: (A) delayed, sectoral choroidal filling; (B) persistent areas of choroidal non-perfusion with early artery sheathing and diffuse capillary dropout; (C) persistent sheathing of the arteries, early optic hyperfluorescence and leakage from parafoveal vessels; (D) late frame showing progressive sheathing, marked leakage, optic nerve hyperfluorescence and hypoperfusion of the choroid and retina.

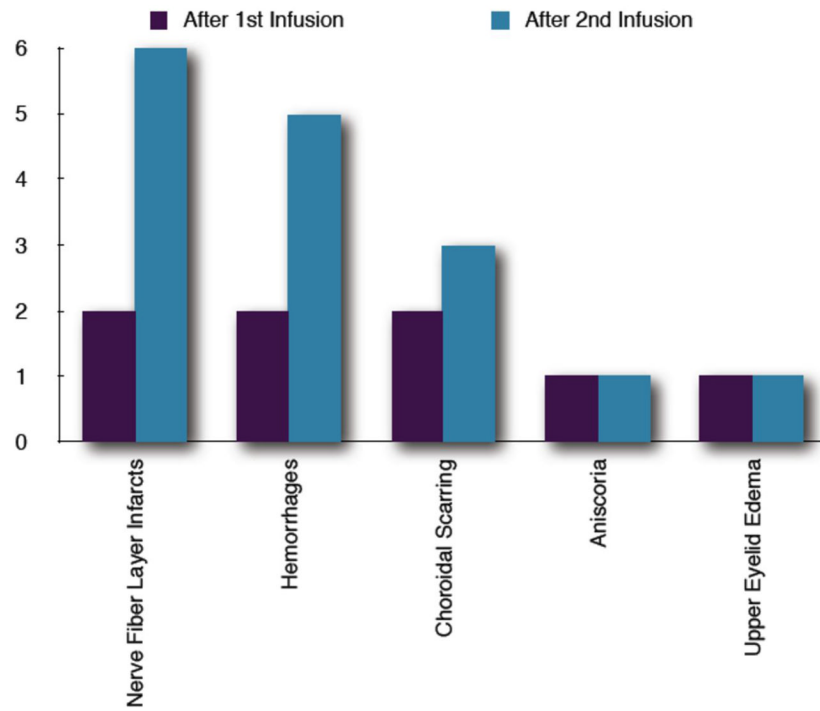


Figure 8. Post-treatment examination findings after first and second infusions. Anisocoria and upper eyelid edema were only seen in the melphanan cohort. One animal showed both anisocoria and upper eyelid edema after the second infusion.

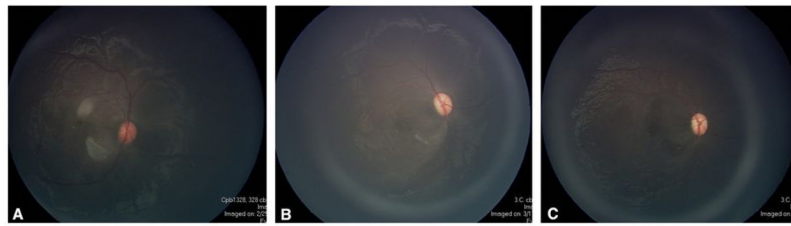


Figure 9. Post-treatment examination of animal in Figures 4 and 7 showing resolution of parafoveal arteriole occlusions with watershed infarcts and resultant retinal atrophy after (A) one week, (B) two weeks, and (C) three weeks.

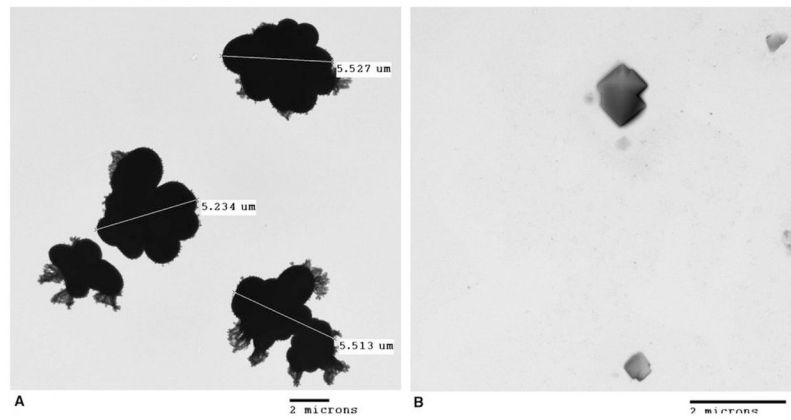


Figure 10. Transmission electron microscopy of (A) melphalan solution (5 mg/30 mL) showing 5 μm particle aggregates and (B) carboplatin solution (30 mg/30 mL) showing 2 μm crystals.

\$watermark-text

\$watermark-text

\$watermark-text

Data collected for each animal including cohort assignment, age, initial and final weights, blood counts after first two infusions, and fluoroscopy time per infusion.

Table 1

Animal	Age (yr)	Initial Weight (kg)	Final Weight (kg)	Infusion	Absolute Neutrophile Count	Hematocrit (%)	Hemoglobin (g/dL)	Fluoroscopy Time (s)
MEL 330	10.5	8.5	8.7	1	4200 (L)	32.4(L)	11.1 (L)	707
				2	4402 (L)	36.8(L)	11.8 (L)	487
				3	*	*	*	243
MEL 006	10.0	13.7	12.8	1	†	†	†	270
				2	8240	36.4(L)	11.8(L)	190
				3	*	*	*	200
MEL 561	22.0+‡	13.7	13.7	1	1219 (L)	41.0	14.2 (L)	841
				2	8295(L)	43.3	13.8	667
				3	*	*	*	545
CBP 328	10.5	13.3	13.9	1	†	†	†	378
				2	2499 (L)	39.2	12.5(L)	638
				3	*	*	*	242
CBP 404	10.0	9.8	10.5	1	1628 (L)	37.0 (L)	11.9 (L)	518
				2	†	†	†	605
				3	*	*	*	790
CBP 039	12.0	9.4	9.5	1	6240	34.2 (L)	11.1 (L)	855
				2	†	†	†	177
				3	*	*	*	576

L = below normal, indicating mild bone marrow suppression.

* Blood counts not measured after third infusion because third infusion was terminal.

† Data not available.

‡ Animal was caught as an adult in 1989, thus actual age unknown.